

# Gap solitons of super-Tonks-Girardeau gas in one-dimensional periodic potential

T. F. Xu<sup>1</sup>, X. L. Jing<sup>1</sup>, H. G. Luo<sup>2,3</sup>, and C. S. Liu<sup>1</sup>

<sup>1</sup>*Department of Physics, Yanshan University, Qinhuangdao 066004, China*

<sup>2</sup>*Center for Interdisciplinary Studies and Key Laboratory for Magnetism and Magnetic Materials of the MoE, Lanzhou University, Lanzhou 730000, China*

<sup>3</sup>*Beijing Computational Science Research Center, Beijing 100084, China*

We study the stability of gap solitons of the super-Tonks-Girardeau bosonic gas in one-dimensional periodic potential. The linear stability analysis indicates that increasing the amplitude of periodic potential or decreasing the nonlinear interactions, the unstable gap solitons can become stable. In particular, the theoretical analysis and numerical calculations show that, comparing to the lower-family of gap solitons, the higher-family of gap solitons are easy to form near the bottoms of the linear Bloch band gaps. The numerical results also verify that the composition relations between various gap solitons and nonlinear Bloch waves are general and can exist in the super-Tonks-Girardeau phase.

PACS numbers: 03.75.Lm, 67.85.-d

## I. INTRODUCTION

The recent development of trapping and cooling techniques enable experimental realizations of low-dimensional ultracold atomic and molecular gases in optical lattices. In particular, by the magnetic Feshbach resonance or confinement-induced resonance methods, the low-dimension particles can be adjusted continually from strong repulsive to attractive interaction. It is therefore possible to realize strongly correlated low-dimensional quantum systems experimentally [1].

For the weakly repulsive regime in one dimension (1D), the degenerate Bose gas acts as a quasi Bose Einstein Condensation (BEC). As the strength of the repulsive interaction tends to infinity, the bosons behave like impenetrable fermions and the system is known as the Tonks-Girardeau (TG) gas [2, 3]. On the contrary, for the strongly attractive regime, the 1D Bose gas is more strongly correlated than the TG gas and can be stable in a wide range of strongly attractive interaction strength, and thus called it as the super Tonks-Girardeau gas (STG) phase [4–6]. The STG gas-like state corresponds to a highly excited states and have no analog in solid-state systems. They can be realized by a sudden quench the effective 1D interaction from the strongly repulsive to the strongly attractive interaction regime by adjusting the magnetism field. The TG gas-like state can transfer into the STG gaslike phase which are hard to realize in traditional condensed-matter physics [7–9]. The existence of these stable gas-like states against cluster-like states due to the existence of large Fermi-pressure-like kinetic energy inheriting from the strongly repulsive interaction. Understanding the dynamic properties of the new synthetic bosonic gas phase is an important subject.

As is well known, the mean-field theory typically does not work well for a 1D system, except in the very weakly interacting regime. The enhanced quantum fluctuation is significant in 1D quantum systems [10–13] which exhibit fascinating phenomena significantly different from their three-dimensional counterparts. Thus when the inter-

action is strong, non-perturbative methods such as the Bose-Fermi mapping [14] or the Bethe ansatz [15, 16] needs to be used to characterize the features of the system properly. In the thermodynamic limit of  $N, L \rightarrow \infty$  and  $N/L$  remains finite, the energy density and chemical potential of Bose gas in TG and STG phase have been extracted from the Bethe-ansatz solution in the absence of the external potential [8, 17]. With the local-density approximation (LDA), a modified nonlinear Schrödinger equation is obtained. Using this kind of nonlinear Schrödinger equation, it is possible to investigate further the dynamic properties of Bose gas in strong interactive regimes.

Associated with the periodicity and nonlinearity, there exist two important waves in nonlinear periodical systems, namely Bloch waves and gap solitons (GSs). Bloch waves, which exist in both linear and nonlinear periodic systems, are extensive and spread over the whole space [18]. On the contrary, GSs, which are spatially localized atomic wave packets, exist only in a nonlinear periodic system [19]. In particular, a class of solitons called the fundamental gap solitons, have the major peak well localized within a unit cell [20]. The solitons with two peaks of opposite signs within a unit cell are called the subfundamental gap solitons [21]. The existence and stability of GSs are important issues. The relationship between the GSs and the nonlinear Bloch waves (NLBWs) is also a topic of considerable interest.

We have studied the GSs and NLBWs of interacting bosons in one-dimensional optical lattices, taking into account the repulsive interaction from the weak to the strong limits [22]. The composition relation between the GSs and NLBWs was verified numerically to exist for the whole span of the interaction strength. The stable GSs was found to form easily in a weakly interacting system with energies near the bottom of the lower-level linear Bloch band gaps. The present issues are whether the stable GSs can exist in the stable STG phase, and whether the composition relation remains valid? To what extent the GSs and NLBWs change when the interaction

changes from repulsive to attractive case?

In this paper, we attempt to investigate the GSs and NLBW of the so-called STG gas in a 1D optical lattices. We are interested particularly in its existences and stability. It will be shown that the amplitude of periodical potential and nonlinear interactions are two important factors for the stability of GSs. The linear stability analysis indicates that stable gap soliton waves is easy to form near the bottoms of the linear Bloch band gaps. The composition relation remains valid in STG phase.

The paper is organized as follows. In Sec. II, we introduce the model equation for a 1D periodic Bose system in STG phase, and then present the Gaussian-like Bose density profile  $\rho(x)$  within a unit cell and chemical potential for different interaction constant  $|c|$  in order to understand the special Bose system from an alternating perspective. In Sec. III, theoretical analysis and numerical simulations are used to investigate the stabilities of different family GSs upon the changes of the interaction and the strength of the periodic potential. We show, in Sec. IV, that the composition relation exists between the NLBW and GSs in the present case. A generalized composition relation between the high-order solitons and multiple periodic waves is also shown in this section. Sec. V is a brief summary.

## II. MODEL EQUATION

We consider a 1D periodic Bose system described by the following modified nonlinear Schrödinger equation

$$\left[ -\frac{\hbar^2}{2m} \frac{d^2}{dx^2} + V_{ext}(x) + \tilde{F}(\rho) \right] \Phi(x) = \mu \Phi(x), \quad (1)$$

where  $V_{ext}(x) = v \cos(\frac{2\pi}{\Lambda}x)$  is the periodic potential with  $\Lambda$  the lattice constant and  $v$  the strength.  $\tilde{F}(\rho)$  is responsible for the interaction energy with  $\rho = |\Phi|^2$ . The nonlinear Schrödinger equation (1) is obtained by a minimization of the free-energy functional  $\mathcal{F} = \mathcal{E} - \mu N$ . The chemical potential  $\mu$  is introduced as a Lagrange multiplier and  $N$  is particle number. The energy functional  $\mathcal{E}$  can be represented as

$$\mathcal{E} = \int dx \left[ \Phi^* \left( -\frac{\hbar^2}{2m} \frac{d^2}{dx^2} + V_{ext} \right) \Phi + \rho \epsilon(\rho) \right]$$

in the LDA where the system is assumed in local equilibrium at each point  $x$  in the external trap. The first gradient term represents additional "local" kinetic energy. The second term is considered as external potential energy. The ground-state energy density can be expressed as  $\epsilon(\rho) = \frac{\hbar^2}{2m} \rho^2 e(\gamma)$ . So  $\tilde{F}(\rho) = \frac{\partial}{\partial \rho} [\rho \epsilon(\rho)]$  with the normalization condition  $\int dx |\Phi(x)|^2 = N$ . The quantum

$$e(\gamma) = \frac{4\pi^2}{3} \frac{1 + p_1|\gamma| + p_2\gamma^2 + p_3|\gamma|^3/4}{1 + q_1|\gamma| + q_2\gamma^2 + p|\gamma|^3} \quad (2)$$

which is obtained by the Bethe-ansatz technique in the attractive STG phase [8]. Here  $\gamma \equiv c/\rho$  with  $c \equiv mg/\hbar^2$

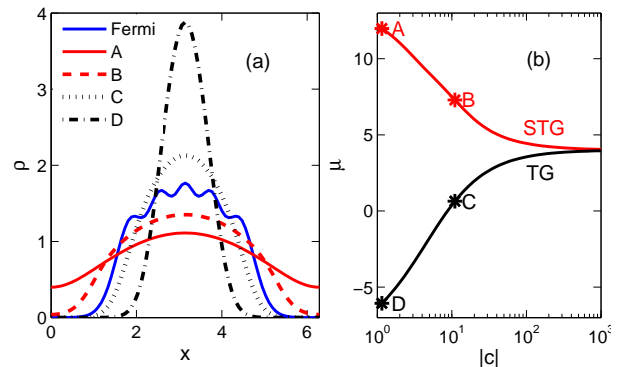


FIG. 1. (Color online) Panel (a): The Gaussian-like Bose density profile  $\rho(x)$  within a unit cell for different interaction constant  $|c|$ . For the repulsive case,  $F(\rho)$  is taken from the Ref. [17]. The density profile labeled by Fermi is obtained by the Bose-Fermi mapping method [22]. The particle number is taken to be 50 and the periodic potential strength is  $v_0 = 10$ . (b) The interaction constant  $|c|$  dependence of chemical potential. The marks A, B, C and D are used to show the parameters which have been used in panel (a).

( $g$  is the scattering length) and  $p_1 = 0.075$ ,  $p_2 = 0.013$ ,  $q_1 = 0.227$ ,  $q_2 = 0.034$ , and  $p = 0.004$  are the fitting parameters. Contrary to the case in repulsive interaction where  $c > 0$ , here  $c < 0$  in the regime from the weak- to the strong attractive interaction of STG phase.

For convenience, dimensionless scaling will be made for the length and the energy. Position  $x$  is to be scaled in the unit of  $\Lambda/(2\pi)$ . Periodic potential  $V_{ext}(x)$ , interaction energy  $\tilde{F}(\rho)$ , and the chemical potential  $\mu$  are all scaled in the unit of  $8E_r$  with  $E_r = \hbar^2\pi^2/2m\Lambda^2$  being the recoil energy. We obtain the following dimensionless time-independent nonlinear Schrödinger equation

$$\left[ -\frac{1}{2} \frac{d^2}{dx^2} + v_0 \cos(x) + F(\rho) \right] \Phi(x) = \mu \Phi(x). \quad (3)$$

Eq. (3) is the starting point of the calculations throughout this paper.

In order to understand Bose gas in the STG phase intuitively, we first compare it to the repulsive interaction case. By solving Eq. (3) numerically to obtain the ground-state density profile  $\rho(x)$  and the corresponding chemical potential  $\mu$  for different interaction constant  $|c|$ . It should note that the transition probability from TG gas to STG phase is low for the weakly attractive regime [7, 8]. In solving Eq. (3), we first differentiate it using the finite-element method along with the periodic boundary condition [23], and then evaluate several hundreds of steps in imaginary time until the lowest chemical potential  $\mu$  is reached. The wave function is then obtained. In fact, the wave function obtained with this method is the NLBW corresponding to the lowest chemical potential  $\mu$ . In the calculation, the system is taken to be 10 lattice constant long ( $x$  ranges from  $-10\pi$  to  $10\pi$ ), the strength of periodic potential  $v = 10$ , and the particle number  $N = 50$  (average 5 particles per unit cell).

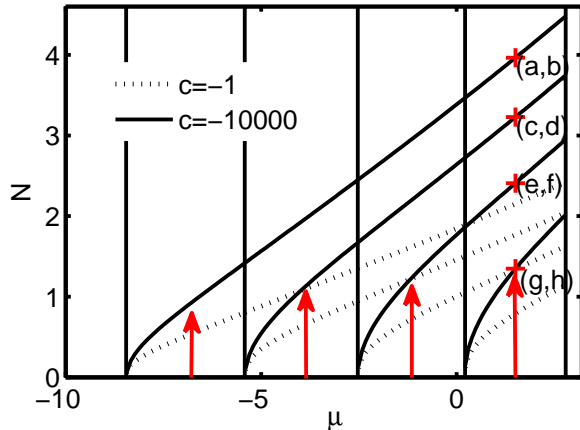


FIG. 2. (Color online) Particle number  $N$  of FGSs as the function of chemical potential  $\mu$  for different interaction constant  $c = -1$  (dotted line),  $-10000$  (solid line) respectively. The points marked by red “+” sign locate at the center of the fourth band gap and will be studied in Fig. 3. The other parameters are same as that in Fig. 1. The arrows indicate the particle number contained in the GSs where the chemical potentials of the GSs are in the center of corresponding band gap.

A Gaussian-like Bose density profile  $\rho(x)$  within a unit cell is shown in Fig. 1(a). When  $|c|$  is increased (see, for example, the case of A and B points shown in Fig. 1(b)), density profile increases at the center while decreases at the two sides. It indicates that Bose gas in STG phase has a larger effective (or equivalent) repulsive interaction in weak attractive regime than that in strong attractive regime if we observe the properties of STG gas only from Eq. 3 and Fig. 1. The existence of large effective (or equivalent) repulsive interaction is, in fact, due to the existence of large kinetic energy inheriting from the strongly repulsive interaction. The repulsive interaction decreases with the increasing of  $|c|$  which is contrast to the case in TG phase (see, for example, the case of C and D). In the extremely strong interaction regime ( $|c| \rightarrow \infty$ ), the chemical potential  $\mu$  of the two phase will coincide in Fig. 1(b) (See also the case B and C approaching the case Fermi in Fig. 1(a)). In such limit, the system will behave similar to the noninteracting fermions. We have used the Bose-Fermi mapping method to calculate the density profile. The five-peak shell structure is shown in Fig. 1(a) (blue solid line). When the large particle number is loaded in the system, a smooth density distribution will emerge.

### III. GAP SOLITONS AND THEIR STABILITIES

#### A. The general features of Gap solitons

We set  $F(\rho) = 0$  to solve the linear Schrödinger equation (3) exactly by the finite-element method. The pe-

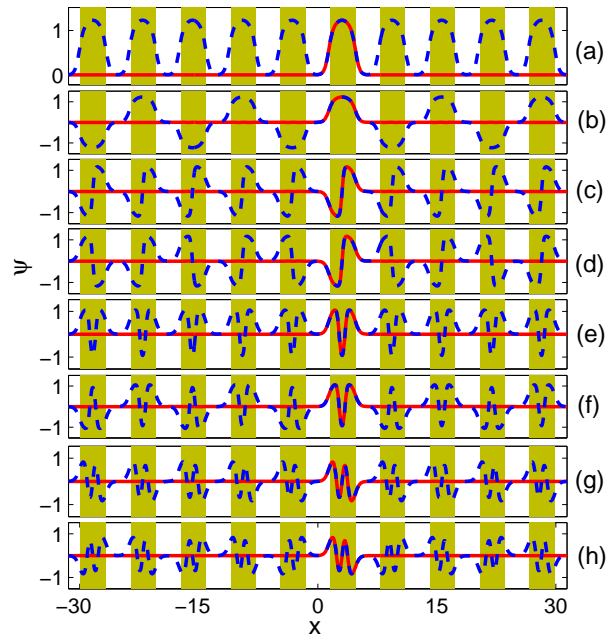


FIG. 3. (Color online) The different family GSs (red solid line) and NLBW (blue dashed line) in the fourth LBB gap marked in Fig. 2.

riodic potential strength  $v_0$ -dependent lowest four bands and band gaps are shown in Fig. 2. A large  $v_0$  is used in our calculations due to the large nonlinear interaction of Bose gas in STG phase. So the Bloch bands reduce to highly-degenerate thin levels. We then retain  $F(\rho)$  to solve the nonlinear Schrödinger equation (3) numerically. The numerical solutions of GSs are obtained by differentiating Eq. (3) on a finite difference grid to obtain a coupled algebraic equations and solve it with the Newton-relaxation method [21].

Figure 2 shows particle number  $N$  of GSs as the function of  $\mu$  for two different interaction constant  $c$ 's. As shown, for example, when  $c = -10000$  close to the strong limit (solid lines), the first nonlinear Bloch band (NLBB) develops from the first linear Bloch band (LBB) and is lifted with the increase of  $N$ . The high-order NLBB develops analogously from the high-order LBB and is lifted with the increase of  $N$ . The so-called NLBB lifting is simply due to the fact that the larger  $N$  is, the larger the nonlinearity and hence the corresponding  $\mu$  are. For weaker interaction case,  $c = -1$  (dotted lines), the NLBB is seen to correspond to less  $N$  for the same  $\mu$ , as compared to those of the  $c = -10000$  case. This is because a large nonlinear interactions correspond to the smaller interaction constant case, one doesn't need a larger  $N$  to achieve the same nonlinear effect.

As shown previously, NLBB can be viewed as the lifted LBB by increasing the nonlinear interaction. While LBB can be viewed as the evolution from the discrete energy levels of an individual well [22, 24]. Therefore it is not difficult to think that NLBW belonging to the  $n$ th

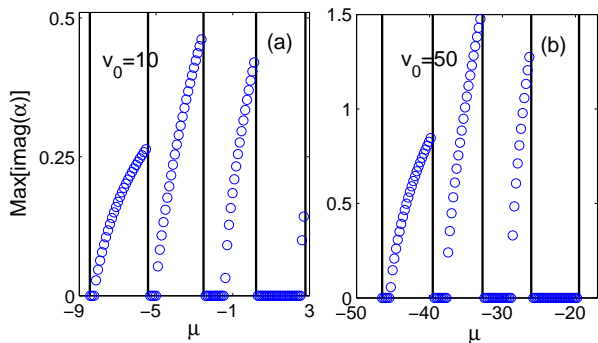


FIG. 4. (Color online) Studies of the stability of the FGSs for different families. The interaction constant  $c = -10000$ . The periodical potentials are taken (a)  $v = 10$  and (b)  $v = 50$  respectively. The other parameters are the same as that used in Fig. 1.

NLBB should have  $n-1$  nodes (in the sense of the  $n$ th bound state) in an individual well of the periodic potential. Therefore, GSs should behave like the bound states in an individual well of the periodic potential in a sense. The different family GSs are presented in Fig. 3. The chemical potentials are all taken in the center of the fourth band gap to show the GSs completely. The GS waves in Fig. 3 (a) and (b) belong to the first family and hence no node. The difference of NLBW between Fig. 3 (a) and (b) is that the later obtain a  $\pi$ -phase difference in adjacent well. The GS waves in Fig. 3 (c) and (d), however, belong to the second family and hence one node. Therefore, the above conclusion remains correct when the nonlinear term is replaced by the  $F(\rho)$  of Bose gap in STG phase.

### B. The stabilities of different family GSs

We shall study the linear stability of various GS solutions in this subsection. As we know, the bright solitons form for atomic matter waves when the linear spreading due to kinetic energy is compensated by the attractive interaction between atoms. Similarly, the existence of GSs is due to that the linear spreading and repulsive atom-atom interaction are compensated by the confinement of periodical potential. It is therefore interesting to study the effect of the nonlinear and periodical potential on the GS stability. Following the standard procedure in Ref. [22], we first add a small perturbation  $\Delta\Phi(x, t)$  to a known solution  $\Phi(x)$ , and then insert the perturbation into Eq. (3). One then obtains the linear eigen equations by dropping the higher-order terms. Among all eigenvalues, if there exists a finite imaginary part, the solution of  $\Phi(x)$  would be unstable. Otherwise, the solution of  $\Phi(x)$  is stable.

The stability of GSs is investigated in Fig. 4 for different amplitude of periodical potential  $v_0 = 10$  and  $v_0 = 50$ . It indicates that the first family GSs which

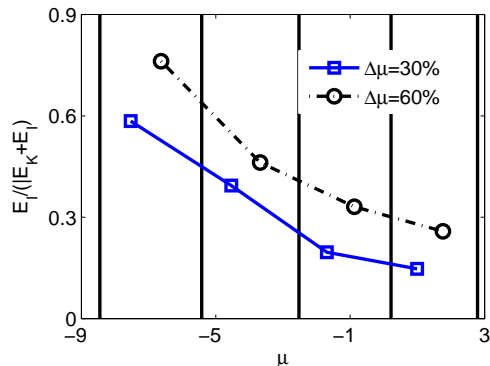


FIG. 5. (Color online) Shown  $\eta(\mu) = E_I / (E_K + E_I)$  for different family GSs. The chemical potentials  $\mu$  are taken 0.3 (blue solid line marked with square) and 0.6 (black dashdot line marked with circle) times band gap width away from the bottom bands respectively. The other parameters are the same as that used in Fig. 4 (a).

develop from the first LBB are stable when their chemical potentials  $\mu$  are near the bottom of the first LBB gap. They will become unstable when  $\mu$  becomes higher within the first band gap (with the increase of  $N$ ), and enters into the second and third band gaps (not shown in Fig. 4). Similarly, the second and high family GSs are also stable when the chemical potentials are near the bottom of the corresponding band gap.

The above behaviors are very similar to the repulsive case. This is due to the little particle number contained in GSs (See Fig. 2) while the GSs develop from the bottoms of band gaps. In such case, the particles behavior is similar to the non-interaction particles in a single potential well. In such case, the GSs are, in fact, the stationary states in discrete energy levels and therefore stable. When increasing the particle number, the interaction between particle will increase. If the interaction energy cannot be compensated by the confinement potential energy when the confinement potential remains unchanged, the GSs will become unstable. Seen also from Fig. 3, the wave functions of high-order family GS have more nodes. It is therefore that the kinetic energy of GS is larger in high-order family than that of in low-order family. From the above analysis, it also indicates the interaction is the main factors to govern the GS stability.

It is interesting to see that the first family GSs are stable only in a narrow regimes near the bottom of the first band gap. This regime becomes wide for high family GSs. See the length of red arrows in Fig. 2, the particle number contained in GSs are equal approximately in the center of band gaps. If judging the GS stability according to the general intuition, the high family GSs should be unstable due to large kinetic energy. In order to understand the GS stability in different family quantitatively, we multiply  $\Phi(x)$  in the left side of Eq. 3 and integrate in whole space to obtain the kinetic energy  $E_K = \int dx |\frac{\partial\Phi(x)}{\partial x}|^2$  and interaction energy between atom

$E_I = \int dx F(\rho)\rho$ . The quantum  $\eta(\mu) = E_I/(E_K + E_I)$  is defined to indicate the effect of repulsive interaction between atoms. The number results of  $\eta(\mu)$  are presented in Fig. 5. The chemical potentials  $\mu$  are taken 0.3 and 0.6 times width of the band gap away from the bottom bands respectively. It is clearly that the repulsive interaction of high family GSs becomes weak relative to the kinetic energy. Therefore, even though with the same particle number, the low-order family GSs are tend to unstable and the high-order family GSs is expected to be stable however.

### C. The effects of periodical potential

Comparing the linear stability analysis presented in Fig. 4 (a) and (b), the fourth family GSs are only unstable in a narrow regime near the top of band gap when  $v_0 = 10$  (Fig. 4 (a)). However, the GSs are all stable in the entire regime of the fourth band gap when  $v_0 = 50$  (Fig. 4 (b)). The increasing of stable regime seems not to be obvious for low-order family GSs when increasing the amplitude of periodical potential.

When increasing periodical potential, the unstable GSs will become stable GSs since the confinement of periodical potential is enough to compensate the linear spreading and repulsive atom-atom interaction. So the stable regime near the bottom of band gap will become wide in such as case. As the above discussions, the effect of non-linear interaction for high-order family GSs are weaker than that of low-order family GSs. It results the variations of the stable regime is obvious for high-order family GSs when increasing the periodical potential. We have also studied the stability of Bose near TG phase numerically. The above behaviors are still right (not present here).

## IV. COMPOSITION RELATIONSHIP

As shown previously, the different family GSs originate from the stable bound state of single periodical well and develop in the band gaps. On the other hand, NLBB can be viewed as the lifted LBB by increasing the nonlinear interaction. However, LBB can be viewed as the evolution from the discrete energy levels of an individual well. Therefore GSs and NLBW should have some similarity. It has shown that GSs and NLBW belonging to the  $n$ th NLBB have  $n-1$  nodes in an individual well of the periodic potential. In particular, it has also pointed out and proven numerically in the whole interaction regime that GSs are the building blocks of the NLBW [22, 24]. The current issue is whether the above statements remain correct when the nonlinear term is replaced by the case of Bose atoms in the STG phase.

In Fig. 3, we have plotted both NLBW (blue dashed line) and GSs (red solid line) for Bose in STG phase ( $c = -10000$ ). An almost perfect (unnoticeable) match

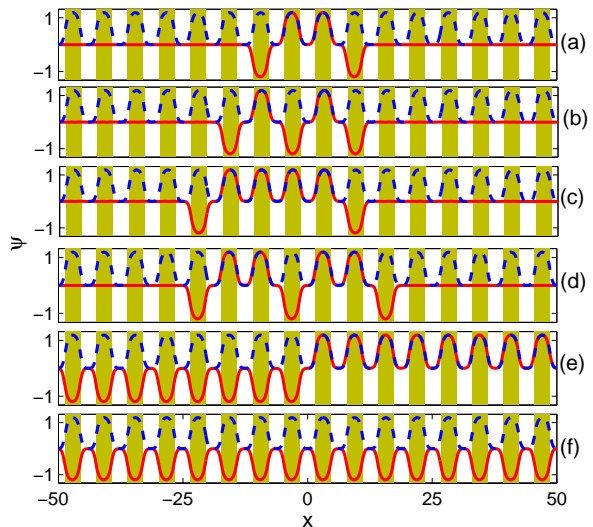


FIG. 6. (Color online) Illustration of the high-order gap solitons (red solid line) and NLBW (blue dashed line) for  $c = -10000$  and  $\mu = 0.20$ . The periodic potential strength is  $v = 10$  for all panels.

is found between the NLBW and the GS within one unit cell. The good match occurs regardless of the first family or the high family GSs. It thus gives a strong evidence that GSs can be considered as the building blocks of the NLBW. It is important to note that the waves shown in Fig. 3(a)&(b) are belonging to the first-family GS and hence of no node. In Fig. 3(c)&(d) however, GS belong to the second-family and hence of one node. The good matches are also found between the NLBW and the GS of high-order family in Fig. 3(e)&(f) and (g)&(h) where multiply nodes exist within one unit cell.

In addition to the GSs and NLBW studied previously, there are two other types of waves which are also common in a nonlinear system. One is called the high-order GSs which are GS waves of multiple peaks over multiple unit cells [25]. Another is called the multiple periodic waves which are defined as  $\Phi(x) = \exp(ikx)\psi_k(x)$  with  $\psi_k(x) = \psi_k(x + 2n\pi)$  and  $n$  being a positive integer [26]. In the repulsive atom interaction, it has been shown that composition relation between the GSs and the NLBW can be generalized to construct multiple periodic waves from the high-order GSs [22, 27]. The present issue is again to see whether the generalized composition relation remains valid in the present case of Bose gas in STG phase.

We have first solved the nonlinear Schrödinger equation (3) numerically using the imaginary-time method with the periodic boundary conditions. The NLBW function  $\Phi(x)$  and chemical potential  $\mu = 0.20$  are obtained accurately with a given interaction constant  $c = -10000$ . The Newton-relaxation method is then used to solve the nonlinear Schrödinger equation (3) to obtain high-order

GSs with the pre-obtained  $\mu = 0.20$  as done in the case of Fig. 3 with the proper guess wave function.

Fig. 6 (a) show the four-peak high-order GSs (two center peaks up, two adjacent peaks down). An almost perfect match is found between the high-order GSs and the NLBW except the phase of wave function in some single well. Thus high-order GSs can also be viewed as the truncated NLBW in the whole interaction regimes. The Newton-relaxation method is further used to solve the nonlinear Schrödinger equation (3) to obtain the multiple periodic waves in Fig. 6 (b) with the pre-obtained  $\mu = 0.20$ . Five periodic high-order GSs in Fig. 6 (b) has been used as the initial guess wave function. An almost perfect match is found between the multiple periodic waves and the NLBW except the phase of wave function in some single well. We also present the multiple periodic waves in Fig. 6 (c) (five-peak periodic waves) and Fig. 6 (d) (ten-peak periodic waves). In particular, we presents twenty-peak periodic waves in Fig. 6 (e). The best matches between GSs and high-order GSs, as well as multiple periodic waves and NLBW, strong support that the GSs are the basic entity and the other waves can built by them.

The above conclusions are useful to obtain NLBW and multiple periodic waves of nonlinear Schrödinger equation. In actual numerical calculation, we can first solve the nonlinear Schrödinger equation to obtain GSs of different family, and then build an initial wave function with the GS. If we want to obtain  $n$ -periodic waves in  $m$ -periodic potential well, the initial guess wave function can be built by  $n$ -GSs as a block ( $m/n$  is assumed to be a integer). If we want to obtain NLBW in  $m$ -periodic potential well, the initial guess wave function can be built by  $m$ -GSs arrangement one by one. With the initial wave

function, the Newton-relaxation method is again used to solve the nonlinear Schrödinger equation (3) to obtain GSs and multiple periodic waves accurately. The advantage of this method is that the initial wave function is very close to the final wave function. The iteration times decrease obviously.

## V. SUMMARY

In summary, we have investigated the GSs of 1D periodic bosonic gas in STG phase. The main focus is to consider its stabilities. By the linear stability analysis, it is found that the periodic potential and the nonlinear interactions are important to the stabilities of GSs. Increasing the amplitude of periodic potential or decreasing the nonlinear interactions, the unstable GSs can turn into stable. It is particular that the high family of GS is easy to form near the bottoms of the LBB gaps. Our numerical results further verify that the composition relation between various GSs and NLBW does exist generally. It gives an alternative way to obtain the NLBW. It is worth emphasizing that the above conclusions are also valid to Bose gas in the whole repulsive interaction regime.

## ACKNOWLEDGMENTS

This work is supported by Hebei Provincial Natural Science Foundation of China (Grant No. A2010001116), and the National Natural Science Foundation of China (Grant No.s 10974169, 11174115, 10934008, 41174116).

- 
- [1] O. Morsch and M. Oberthaler, *Rev. Mod. Phys.* **78**, 179 (2006).
  - [2] L. Tonks, *Phys. Rev.* **50**, 955 (1936).
  - [3] M. D. Girardeau, *J. Math. Phys. (NY)* **1**, 516 (1960).
  - [4] G. E. Astrakharchik, J. Boronat, J. Casulleras, and S. Giorgini, *Phys. Rev. Lett.* **95**, 190407 (2005).
  - [5] M. T. Batchelor, M. Bortz, X. W. Guan, and N. Oelkers, *J. Stat. Mech.* **2005**, L10001 (2005).
  - [6] E. Tempfli, S. Zöllner, and P. Schmelcher, *New Journal of Physics* **10**, 103021 (2008).
  - [7] E. Haller, M. Gustavsson, M. J. Mark, J. G. Danzl, R. Hart, G. Pupillo, and H.-C. Nägerl, *Science* **325**, 1224 (2009).
  - [8] S. Chen, L. Guan, X. Yin, Y. Hao, and X.-W. Guan, *Phys. Rev. A* **81**, 031609 (2010).
  - [9] Y. Hao, H. Guo, Y. Zhang, and S. Chen, *Phys. Rev. A* **83**, 053632 (2011).
  - [10] E. H. Lieb and W. Liniger, *Phys. Rev.* **130**, 1605 (1963).
  - [11] D. S. Petrov, G. V. Shlyapnikov, and J. T. M. Walraven, *Phys. Rev. Lett.* **85**, 3745 (2000).
  - [12] V. Dunjko, V. Lorent, and M. Olshanii, *Phys. Rev. Lett.* **86**, 5413 (2001).
  - [13] S. Chen and R. Egger, *Phys. Rev. A* **68**, 063605 (2003).
  - [14] M. D. Girardeau and A. Minguzzi, *Phys. Rev. Lett.* **99**, 230402 (2007).
  - [15] B. Sutherland, *Phys. Rev. Lett.* **20**, 98 (1968).
  - [16] Y.-Q. Li, S.-J. Gu, Z.-J. Ying, and U. Eckern, *EPL (Europhysics Letters)* **61**, 368 (2003).
  - [17] Y. Hao and S. Chen, *Phys. Rev. A* **80**, 043608 (2009).
  - [18] N. W. Ashcroft and N. D. Mermin, *Solid State Physics* (1976).
  - [19] Y. Kivshar and G. Agrawal, *From Fibers to Photonic Crystals* (2003) p. 540.
  - [20] P. J. Y. Louis, E. A. Ostrovskaya, C. M. Savage, and Y. S. Kivshar, *Phys. Rev. A* **67**, 013602 (2003).
  - [21] T. Mayteevarunyoo and B. A. Malomed, *Phys. Rev. A* **74**, 033616 (2006).
  - [22] T. F. Xu, X. M. Guo, X. L. Jing, W. C. Wu, and C. S. Liu, *Phys. Rev. A* **83**, 043610 (2011).
  - [23] C. Johnson, *Numerical Solution of Partial Differential Equations by the Finite Element Method*, (Studentlitteratur, Lund, Sweden, 1987).
  - [24] Y. Zhang and B. Wu, *Phys. Rev. Lett.* **102**, 093905 (2009).

- [25] J. Wang, J. Yang, T. J. Alexander, and Y. S. Kivshar, Phys. Rev. A **79**, 043610 (2009).
- [26] M. Machholm, A. Nicolin, C. J. Pethick, and H. Smith, Phys. Rev. A **69**, 043604 (2004).
- [27] Y. Zhang, Z. Liang, and B. Wu, Phys. Rev. A **80**, 063815 (2009).